Langmuir

Article

pubs.acs.org/Langmuir

Microfluidic Generation of Polydopamine Gradients on Hydrophobic Surfaces

Xuetao Shi,[†,∥] Serge Ostrovidov,[†,∥] Yiwei Shu,[‡] Xiaobin Liang,[†] Ken Nakajima,[†] Hongkai Wu,*[,†,‡] and Ali Khademhosseini*[,†,§,⊥]

[†]WPI-Advanced Institute for Materials Research, Tohoku University, Sendai 980-8578, Japan

[‡]Department of Chemistry & Division of Biomedical Engineering, Hong Kong University of Science & Technology, Hong Kong, China

[§]Center for Biomedical Engineering, Department of Medicine, Brigham and Women's Hospital, Harvard Medical School; Harvard-MIT Division of Health Sciences and Technology Massachusetts Institute of Technology; Wyss Institute for Biologically Inspired Engineering at Harvard University, Boston, Massachusetts 02115, United States

[⊥]Department of Maxillofacial Biomedical Engineering and Institute of Oral Biology, School of Dentistry, Kyung Hee University, Seoul 130-701, Republic of Korea

Supporting Information

ABSTRACT: Engineered surface-bound molecular gradients are of great importance for a range of biological applications. In this paper, we fabricated a polydopamine gradient on a hydrophobic surface. A microfluidic device was used to generate a covalently conjugated gradient of polydopamine (PDA), which changed the wettabilty and the surface energy of the substrate. The gradient was subsequently used to enable the spatial deposition of adhesive proteins on the surface. When seeded with human adipose mesenchymal stem cells, the PDA-graded surface induced a gradient of cell adhesion and spreading. The PDA gradient developed in this study is a promising tool for controlling cellular behavior and may be useful in various biological applications.

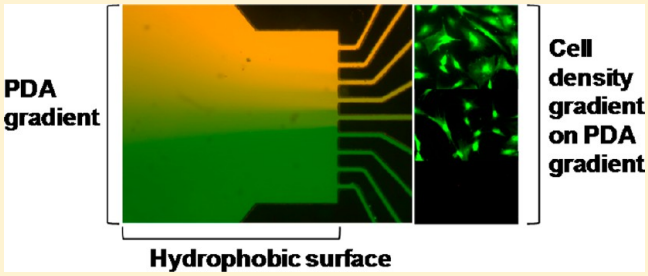

1. INTRODUCTION

Gradients are important in a number of biological processes including chemotaxis, embryogenesis, wound healing, metastasis, and inflammation.[1−3] These biological processes can be studied *in vitro* to study various cell behaviors, such as cell attachment, growth, and differentiation, under molecular gradients.[4−9] However, precise molecular gradients with temporal and spatial stability are difficult to generate. Numerous approaches have been developed to construct various biomolecular, chemical, or mechanical gradients.[10,11] Among them, microfluidic gradient generators are based on the diffusive mixing of continuous flow streams that carry different concentrations of a substance. Such systems (e.g., the T-sensor, tree-shaped microfluidic mixer, or multigradient generator) provide precise control of the gradient stability, size, and shape.[12−14] However, they are not adapted for addressing biological questions when the regulation of the cellular behavior is mediated by autocrine/paracrine-soluble factors.[15] To overcome this limitation and to enable the generation of gradients in static solution, gradient generators based on diffusion through a membrane or hydrogel between a source and sink have been developed.[16] Although a hydrogel slab can retain the molecular gradient shape for a long time, common hydrogels for cell encapsulation or culture, such as agarose or alginate hydrogels, are inert and do not induce cell adhesion and cell spreading.[17] Therefore, generating an immobilized gradient of functional molecules on the surface of materials to regulate cell behavior is of benefit.

Fabricating surface-bound gradients on hydrophobic materials is important for both interface tissue regeneration and tissue culture applications. In particular, many types of materials such as poly(caprolactone), poly(lactic-*co*-glycolic acid) (PLGA), and poly(dimethylsiloxane) (PDMS), that are commonly used for *in vivo* implantation or *in vitro* cell culture, possess a hydrophobic surface. Furthermore, many such materials lack functional groups that can effectively induce protein immobilization or cell adhesion.[18−20] Therefore, we postulated that coating such synthetic materials with a PDA gradient would allow us to build a graded surface by immobilizing functional molecules. PDA is an eumelanin polymer which is derived from dopamine (a small molecule in the catecholamine family and a key neurotransmitter).[21,22] One of the impressive properties of PDA is that it can be deposited on various hydrophilic or hydrophobic surfaces in different shapes via facile self-

Received: October 28, 2013
Revised: December 19, 2013
Published: December 20, 2013

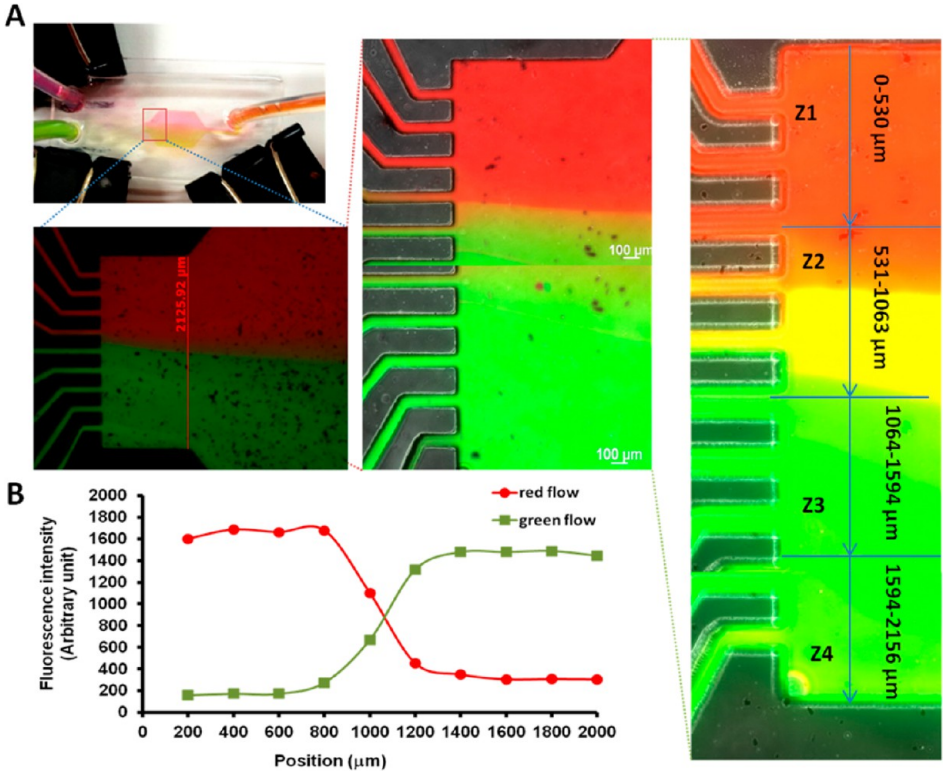

Figure 1. Gradient generation in the microfluidic device. (A) Image of the red and green dyes flowing in the microfluidic device. There was 1% rhodamine B in red dye for one inlet and 1% FITC-dex in green dye for the other inlet. (B) Fluorescence intensity profiles in different zones of the chamber.

polymerization by oxidation of the dopamine in a weak alkaline buffer solution (pH value of around 8.5).[23,24] PDA coatings have excellent biocompatibility, which can promote cell adhesion and proliferation.[25] Furthermore, PDA coatings also facilitate the immobilization and conjugation of various proteins and enzymes.[26,27]

Microfluidic systems can be used to generate chemical/physical gradients that go beyond conventional gradient generators, such as Boyden and Zigmond chambers.[16,28,29] Herein, we present a facile method of fabricating surface-bound PDA and protein gradients on a hydrophobic surface by using a microfluidic device. This system was used to study stem cell adhesion and morphology in response to PDA gradients. Due to the versatility of PDA in inducing protein immobilization and cell adhesion, the developed PDA graded surfaces may provide an alternative approach to create protein or cell gradients on the surface of hydrophobic biomaterials for tissue engineering applications.

2. EXPERIMENTAL SECTION

Materials. Polydimethylsiloxane (PDMS) and curring agent were purchased from Dow Corning Toray, Japan. Glass slides were purchase from Matsunami, Tokyo, Japan. Trichloro (1*H*,1*H*,2*H*,2*H*-tridecafluoro-*n*-octyl) silane (FOTS) was purchased from Tokyo Chemical Industry, Japan. Dopamine hydrochloride was purchased from Sigma-Aldrich, USA. Tris(hydroxymethyl) aminomethane (Tris) was purchased from AMRESCO, USA. The syringe pump (Aladdin syringe pump) was purchased from World Precision Instruments, Sarasota, FL, USA. Adipose derived mesenchymal stem cells (ADMSCs) were purchased from DS Pharm Biomedical, Osaka, Japan. Culture medium (Dulbecco's modified Eagle's medium (DMEM)/F12), streptomycin/penicillin, and fetal bovine serum (FBS) were purchased from Invitrogen, Tokyo, Japan. Rhodamine, fluorescein isothiocyanate labeled bovine serum albumin (FITC-BSA), and fluorescein isothiocyanate-dextran (FITC-dex) were purchased from Sigma-Aldrich (USA).

Device Fabrication. Microfluidic devices were fabricated by using soft lithography.[30−33] The SU-8 master mold consists of a microfluidic mixer (12 × 10 × 0.18 mm^3) coupled to a chamber (7.2 × 7.2 × 0.18 mm^3) (Figure 1). To fabricate the microstructured PDMS layer, PDMS prepolymer was homogenized with the curing agent (10:1 (w/w)), poured into a SU-8 mold, and cured in an oven at 70 °C for 1.5 h. The PDMS layer was peeled off from the SU-8 mold, and holes were made at the inlets and outlet with a biopsy punch. Two bands of tape (5 mm wide) were taped on the borders of a glass slide and used to mask these surface portions. The glass slide was then silanized with perfluoro-octyltrichlorosilane (FOTS) vapor for 1 h in a vacuum chamber to obtain a hydrophobic surface. After removing the tape, we used a piece of plastic film to cover the area on the glass slide that corresponded to the PDMS chamber to protect the silane coating. The PDMS layer and glass slide were then subjected to an O_2 plasma in a plasma cleaner (Harrick Plasma, model PDC-001) for 10 s. The PDMS layer was then bonded permanently to the glass slide, and silicon tubes were fixed at the inlets and outlet.

Generation of PDA Gradients. A microfluidic device was used to create a gradient of PDA in the chamber. A solution of dopamine hydrochloride (0.2% in Tris 10 mM pH 8.5) was injected in one inlet, while a 10 mM, pH 8.5 Tris solution was injected in the other inlet. Both solutions were flowed through the channel for 8 h at 3 μL/min with a syringe pump (KD Scientific, 78-KDS200E), and both solution containers were refilled with fresh solutions after the first 4 h. Subsequently, the device was opened by removing the PDMS layer with a scalpel. The glass slide, which presented a black PDA gradient, was rinsed gently with Milli-Q water and then placed in a culture dish under a clean bench for UV sterilization for 15 min. The generated PDA gradient was analyzed by a phase contrast microscope (Zeiss, Germany) and atomic force microscope (AFM).

Protein Immobilization. A 1% fluorescein isothiocyanate-bovine serum albumin (FITC-BSA) solution (in DI water) was added to the

dx.doi.org/10.1021/la4041216 | *Langmuir* 2014, 30, 832−838

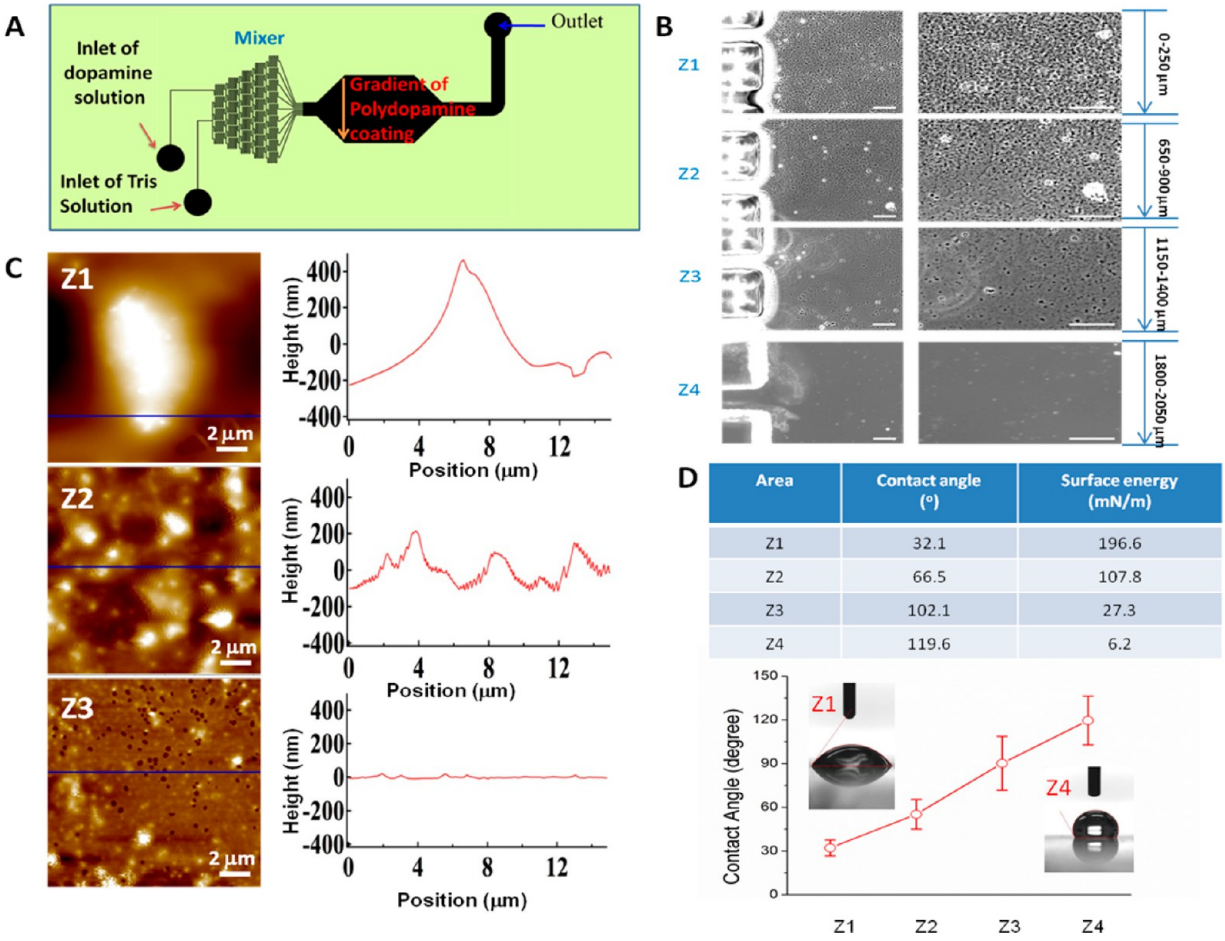

Figure 2. Generation of a PDA gradient in the microfluidic device. (A) Schematic of the microfluidic device used to generate the PDA gradient. (B) Phase contrast images of the PDA deposition in different zones of the chamber. (C) Height images of the PDA deposition in different zones of the chamber obtained by atomic force microscopy (AFM) using tapping mode and corresponding sectional analysis (scan size is 15 μm). (D) Contact angles and surface energy of the PDA gradient surface. Scale bars are 50 μm.

slide with the PDA gradient, and then the slide was incubated at 37 °C for 3 h. Afterward, the slide was washed with DI water three times. The immobilized FITC-BSA was imaged using a fluorescence microscope (Axio Observer, Zeiss, Germany). The degree of fluorescence of the protein was quantified and analyzed using Image J.

Atomic Force Microscope (AFM) Measurement. AFM measurements were carried out on a commercial Bruker MultiMode system (Bruker Corp. US) with a NanoScope V controller under ambient conditions. In tapping mode AFM, we used silicon cantilevers (OMCL-AC160TS-R3) with resonance frequencies of f_0 ~300 kHz and a nominal spring constant of 20–30 N/m. A moderate tapping force corresponding to a force of ~1 nN was used.

Cell Seeding and Proliferation. ADMSCs were cultured in DMEM/F12 supplemented with 1% streptomycin/penicillin and 10% (v/v) FBS. The sterilized slide containing a PDA gradient (using UV light for 30 min each side) was loaded with 100 μL of a solution containing ADMSCs (DS Pharm Biomedical Inc., Osaka, Japan) at a concentration of 5×10^5 cells/mL and cultured in an incubator at 37 °C and 5% CO_2. The cells were analyzed using Live/Dead assay (Invitrogen, green (live)/red (dead)) as well as staining for rhodamine-phalloidin (for F-actin, Invitrogen) and DAPI (for nuclei, Invitrogen). Five images from three individual samples for each sample type were analyzed for cell number (by counting cell nuclei in each image). To quantify cell spreading, the cell surface coverage (area of fluorescence produced by stained cells) was measured by using ImageJ software. The average area per cells was calculated by dividing the cell surface coverage by the cell number.

3. RESULTS AND DISCUSSION

A variety of methods have been developed to generate surface gradients using microfluidics.[34] In this study, we use a microfluidic mixer based on a tree-shaped microfluidic network, which repeatedly splits the streams and mixes them by diffusion.[13] At the end of the microfluidic network, the gradient is generated perpendicular to the flow. This system allows for the generation of different gradient types (e.g., smooth, step, multipeak) in a range of sizes.[14] In a previous study, we used this type of system to generate a concentration gradient of a drug.[35] To investigate the gradient generation, we generated a double-crossing step gradient (Figure 1 and Figure S1, Supporting Information) by injecting two different fluorescent dye solutions in the device. The analysis of the fluorescence intensities at the inlet of the chamber exhibited three sections in the intensity profiles of rhodamine (red) and FITC-dex (green). In the top section, from 200 to 800 μm, the rhodamine intensity is high, whereas the FITC-dex intensity is low. In the middle section, from 800 to 1400 μm, the rhodamine intensity decreases gradually, whereas the FITC-dex intensity increases. In the bottom section, from 1400 to 2000 μm, the rhodamine intensity is low, whereas the FITC-dex intensity is high. We therefore divided the chamber into four different zones (Z1, Z2, Z3, and Z4) from 0 to 2000 μm.

dx.doi.org/10.1021/la4041216 | Langmuir 2014, 30, 832–838

After confirming the formation of the various zones containing different concentrations of the two inlet solutions, we used this system to generate a PDA gradient on a hydrophobic surface, which acts as the substrate of the fluidic chamber. First, to generate a hydrophobic surface on a glass slide, a fluoroalkylsilane layer was precoated onto the glass slide's surface. The PDA gradient was generated by replacing the two different fluorescent dye solutions in the aforementioned experiment with a dopamine Tris solution (pH 8.5) and Tris buffer (pH 8.5), respectively (Figure 2A). The dopamine solution and Tris buffer continuously flowed inside the devices for 8 h with a flow rate of 3 μL/min. The dopamine solution was changed after 4 h to replenish the dopamine solution because of continuous conversion of dopamine to PDA. During the PDA gradient generation, the dopamine self-polymerization and PDA deposition were visible through a distinct surface color change in the chamber. After 3−4 h, the upper section of the chamber, where the dopamine solution was flowing, exhibited a darker greyish color. As expected, the intensity of this color increased with longer reaction times. After 8 h, the fluid flow was stopped and the residual solution was carefully removed. A PDA gradient was clearly visible on the surface of the hydrophobic fluoroalkylsilane-treated glass slide (Figures S2 and S3, Supporting Information). The dark gray color in the upper section indicated the deposition of PDA, whereas the bottom section retained its original color. To further investigate the PDA gradient generation, we used an optical microscope and AFM to observe the morphology of the PDA deposition. As shown in Figure 2B and C, black dots denoting PDA aggregations (bulges in AFM images) were clearly observed in Z1 and Z2 regions. In the Z4 regions, almost no PDA aggregates were observed because no dopamine solution flowed in this area. The PDA aggregations gradually decreased from Z1 to Z4.

Upon formation of the PDA gradient, the surface properties of the hydrophobic fluoroalkylsilane-treated glass slide were noticeably changed. We performed a static water contact angle test to measure the wettability of the generated PDA-graded surface (Figure 2D). In Z1 and Z4, the water contact angles were 32.1 and 119.6°, and the surface energies were 196.56 and 6.22 mN/m, respectively, indicating that the PDA coating can enhance the hydrophilicity and the surface energy of the substrate. In Z2 and Z3, the contact angles were approximately 52 and 90°.

One of the most important processes for cell adhesion on artificial materials is the deposition of extracellular matrix (ECM) (e.g., collagen, laminin, and fibronectin). The process of protein deposition on an artificial surface is either directly mediated by cells depositing matrix on a surface or occurs through adsorption of proteins from the cell culture medium.[36] To evaluate the immobilization of proteins on the PDA gradient, we immersed the glass slide with a PDA gradient into a protein solution. For the present study, FITC-BSA was used as a model protein, as albumin is the most abundant protein in the serum. After 3 h of incubation in a solution containing 1% FITC-BSA, the glass slide with a PDA gradient was rinsed and dried. Figure 3A shows the fluorescence microscopy images of the FITC-BSA immobilization on the PDA gradient. A visible FITC-BSA gradient was visible on the PDA gradient surface with the fluorescence intensity decreasing along the PDA gradient. Higher fluorescence intensity was observed in the area with a higher density of the PDA coatings. In contrast, as the PDA coating decreased, the fluorescence intensity of FITC-BSA also decreased (Figure 3B). No fluorescence could be observed in the area of the slide where almost no PDA was deposited (Z4). In addition to BSA, PDA coatings also facilitate the conjugation of various biomacromolecules including peptides, proteins, and growth factors.[37−39] For instance, to induce the osteogenic commitment of stem cells, Arg-Gly-Asp peptides and bone morphogenetic protein-2 were immobilized onto polydopamine coated titanium implants.[40] To promote osteogenesis, PDA can assist hydroxyapatite deposition onto bioceramics, biometals, and synthetic polymers.[41] Additionally, trypsin can also be immobilized by the assistance of PDA for inducing protein digestion.[42]

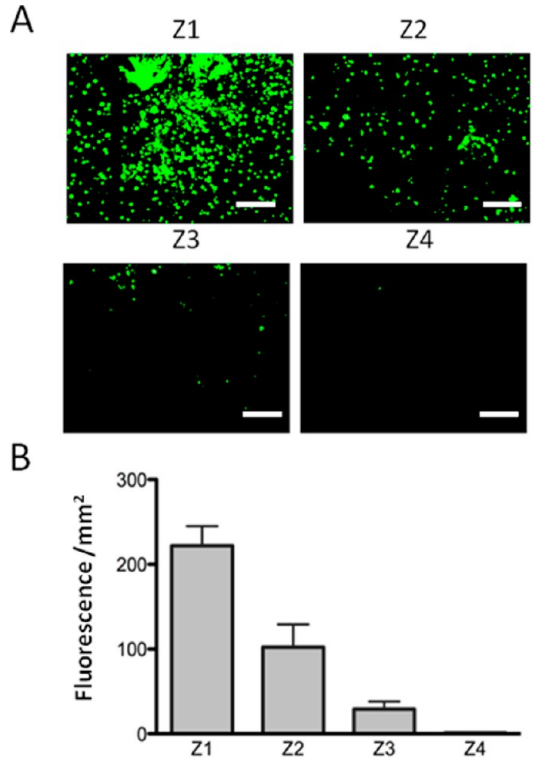

Figure 3. Protein immobilization on the glass slide with a PDA gradient. (A) Fluorescence images of FITC-BSA immobilization on the different zones of the glass slide with a PDA gradient. (B) Fluorescence area (the area of fluorescence clusters in a zone). Scale bars are 100 μm.

We then investigated if a cell gradient could be generated on the PDA gradient surface according to the conceived concept. Mesenchymal stem cells derived from human adipose tissue (ADMSCs) were seeded on the PDA gradient surface. The cells on the surface were stained with a live (green)/dead (red) assay as well as for rhodamine phalloidin (for F-actin) and DAPI (for cell nuclei) after 2 days of culture (Figure 4A). The quantification of the cell number, cell surface coverage, and average area per cell were evaluated (Figure 4B, C, and D). In Z1, the cells were fully spread, with many cells exhibiting a polygonal morphology. In Z2, most cells had a fibroblast-like morphology, and the average cell size was significantly decreased; however, there was only a slight decrease in the cell numbers in this area when compared with Z1. In Z3, only a few cells attached on the upper side. In contrast, no cells were observed on the bottom side of Z3 and in Z4, indicating that the hydrophobic fluoroalkylsilane treated glass slide inhibited cell adhesion. Furthermore, the cells in Z3 were less spread than those in Z1 and Z2. Additionally, the amount of F-actin in

dx.doi.org/10.1021/la4041216 | Langmuir 2014, 30, 832−838

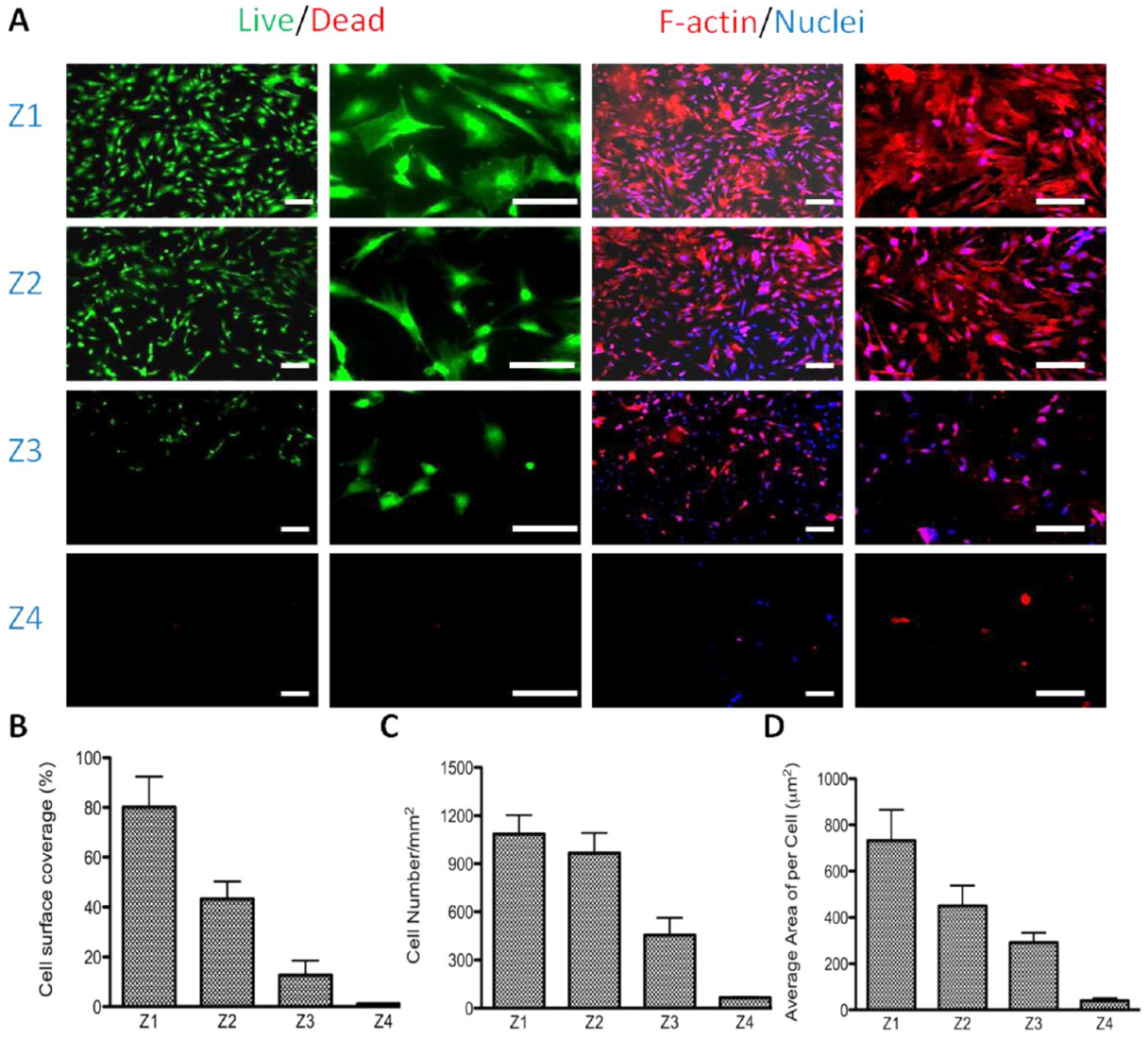

Figure 4. Cell adhesion on the glass slide with a PDA gradient. (A) Live/dead and F-actin/nuclei staining of cells. (B) Cell surface coverage. (C) Cell number. (D) Average area per cell (cell area divided by the cell number). Scale bars are 100 μm.

the cells gradually decreased from Z1 to Z4. This difference in cell morphology along the gradient is correlated with the decrease of wettability from Z1 to Z4 induced by the PDA gradient. Taken together, these results indicated that the PDA gradient not only regulates cell adhesion but also affects cell morphology. Previous studies have indicated that PDA coatings increase the adhesion of various cell lineages.[43−45] This cell adhesion enhancement is attributed to the amine and thiol groups of bioactive molecules (e.g., cell adhesive proteins or peptides, and growth factors) which can be covalently conjugated via the quinine group of PDA coatings.[46] In this study, from Z1 to Z4, the cell number and cell spreading gradually decreased. This phenomenon is due to good cell adhesion on the PDA coating in Z1 and Z2, while the hydrophobic surface in Z3 and Z4 decreases cell adhesion. It is acknowledged that surface wettability of artificial materials is one of most important factors determining cell adhesion and materials with water contact angles around 30−70° facilitate cell adhesion.[47]

Compared with the conventional techniques for generating surface-bound molecular and cellular gradients,[48] the method developed here has considerable advantages. Indeed, bio-molecular surface gradients are usually generated from non-covalent[49] or covalent reactions.[50] If gradients formed by covalent bonding are stable over time, they usually require complex coupling strategies,[51] which may inactivate the biological function of the molecule. In contrast, gradients formed by non-covalent methods such as physical adsorption or affinity immobilization are not stable over time.[52] PDA tightly adhered on the surface of the substrate via both covalent and non-covalent interactions.[26,53,54] Advantageously, PDA gradients are stable over time, easy to form by simple immersion, and enable stable protein immobilization by conjugation.[23] Furthermore, this process is compatible with other gradient generation techniques (e.g., organosilane based methods,[55] microfluidics,[2] and photopatterning[56]). In addition, whereas other processes may be suitable for only certain types of surfaces,[57] a PDA gradient can be generated on various hydrophobic and hydrophilic materials, including polymers, ceramics, and metals, by following the same protocol.[26,58] A PDA coating can even be created on the surface of Teflon, which is unique for its nonstick properties.[26] Given these merits, PDA gradients have significant promise in a range of different applications.

dx.doi.org/10.1021/la4041216 | *Langmuir* 2014, 30, 832−838

4. CONCLUSIONS

In summary, we demonstrated an innovative and facile format for creating a stable PDA gradient by self-polymerization and biomicrofluidic techniques. The generated PDA gradient can efficiently induce protein immobilization and regulate cell adhesion. This simple technology not only offers new possibilities for developing gradient biomaterials for interface tissue repair but also provides a new platform for investigating cell behavior in response to gradients in biochemical cues.

■ ASSOCIATED CONTENT

Ⓢ Supporting Information

A detailed schematic of the microfluidic device for gradient generation and photo plus SEM pictures of the polydopamine gradient obtained. This material is available free of charge via the Internet at http://pubs.acs.org.

■ AUTHOR INFORMATION

Corresponding Authors

*E-mail: chhkwu@ust.hk (H.W.).

*E-mail: alik@rics.bwh.harvard.edu (A.K.).

Author Contributions

‖These authors contributed equally to this work.

Author Contributions

X.S. and S.O. conceived the project, performed the experiments, analyzed the results, and wrote the manuscript. X.L. made the AFM measurements under the supervision of K.N. H.W. and A.K. supervised the whole project. All authors have read the manuscript, commented on it, and have given approval to the final version of the manuscript.

Notes

The authors declare no competing financial interest.

■ ACKNOWLEDGMENTS

This work was supported by WPI-Initiative funding from the Japan Society for the Promotion of Science and the Ministry of Education, Culture, Sports, Science and Technology, Japan. H.W. acknowledges support from Hong Kong RGC (GRF 604712 and GRF 605210).

■ REFERENCES

(1) Zigmond, S. H. Mechanisms of sensing chemical gradients by polymorphonuclear leukocytes. *Nature* **1974**, *249*, 450−452.

(2) Keenan, T. M.; Folch, A. Biomolecular gradients in cell culture systems. *Lab Chip* **2008**, *8*, 34−57.

(3) Wong, J. Y.; Velasco, A.; Rajagopalan, P.; Pham, Q. Directed movement of vascular smooth muscle cells on gradient-compliant hydrogels. *Langmuir* **2003**, *19*, 1908−1913.

(4) Li, X.; Xie, J.; Lipner, J.; Yuan, X.; Thomopoulos, S.; Xia, Y. Nanofiber scaffolds with gradations in mineral content for mimicking the tendon-to-bone insertion site. *Nano Lett.* **2009**, *9*, 2763−2768.

(5) Sundararaghavan, H. G.; Saunders, R. L.; Hammer, D. A.; Burdick, J. A. Fiber alignment directs cell motility over chemotactic gradients. *Biotechnol. Bioeng.* **2013**, *110*, 1249−1254.

(6) Liu, W.; Zhang, Y.; Thomopoulos, S.; Xia, Y. Generation of controllable gradients in cell density. *Angew. Chem., Int. Ed.* **2013**, *52*, 429−432.

(7) Seidi, A.; Ramalingam, M.; Elloumi-Hannachi, I.; Ostrovidov, S.; Khademhosseini, A. Gradient biomaterials for soft-to-hard interface tissue engineering. *Acta Biomater.* **2011**, *7*, 1441−1451.

(8) Seidi, A.; Kaji, H.; Annabi, N.; Ostrovidov, S.; Ramalingam, M.; Khademhosseini, A. A microfluidic-based neurotoxin concentration gradient for the generation of an in vitro model of Parkinson's disease. *Biomicrofluidics* **2011**, *5*, 022214−14.

(9) Shi, X.; Zhou, J.; Zhao, Y.; Li, L.; Wu, H. Gradient-regulated hydrogel for interface tissue engineering: Steering simultaneous osteo/chondrogenesis of stem cells on a chip. *Adv. Healthcare Mater.* **2013**, *2*, 846−853.

(10) Trappmann, B.; Gautrot, J. E.; Connelly, J. T.; Strange, D. G. T.; Li, Y.; Oyen, M. L.; Cohen Stuart, M. A.; Boehm, H.; Li, B.; Vogel, V.; Spatz, J. P.; Watt, F. M.; Huck, W. T. S. Extracellular-matrix tethering regulates stem-cell fate. *Nat. Mater.* **2012**, *11*, 642−649.

(11) Moore, M.; Moore, R.; McFetridge, P. S. Directed oxygen gradients initiate a robust early remodeling response in engineered vascular grafts. *Tissue Eng., Part A* **2013**, *19*, 2005−2013.

(12) Kamholz, A. E.; Weigl, B. H.; Finlayson, B. A.; Yager, P. Quantitative analysis of molecular interaction in a microfluidic channel: The T-sensor. *Anal. Chem.* **1999**, *71*, 5340−5347.

(13) Jeon, N. L.; Dertinger, S. K. W.; Chiu, D. T.; Choi, I. S.; Stroock, A. D.; Whitesides, G. M. Generation of solution and surface gradients using microfluidic systems. *Langmuir* **2000**, *16*, 8311−8316.

(14) Dertinger, S. K. W.; Chiu, D. T.; Jeon, N. L.; Whitesides, G. M. Generation of gradients having complex shapes using microfluidic networks. *Anal. Chem.* **2001**, *73*, 1240−1246.

(15) Abhyankar, V. V.; Lokuta, M. A.; Huttenlocher, A.; Beebe, D. J. Characterization of a membrane-based gradient generator for use in cell-signaling studies. *Lab Chip* **2006**, *6*, 389−393.

(16) Wu, H.; Huang, B.; Zare, R. N. Generation of complex, static solution gradients in microfluidic channels. *J. Am. Chem. Soc.* **2006**, *128*, 4194−4195.

(17) Kirschner, C. M.; Anseth, K. S. Hydrogels in healthcare: From static to dynamic material microenvironments. *Acta Mater.* **2013**, *61*, 931−944.

(18) Zhou, J.; Ellis, A. V.; Voelcker, N. H. Recent developments in PDMS surface modification for microfluidic devices. *Electrophoresis* **2010**, *31*, 2−16.

(19) Shi, X.; Wang, Y.; Ren, L.; Lai, C.; Gong, Y.; Wang, D.-A. A novel hydrophilic poly(lactide-co-glycolide)/lecithin hybrid microspheres sintered scaffold for bone repair. *J. Biomed. Mater. Res., Part A* **2010**, *92A*, 963−972.

(20) Shi, X.; Chen, S.; Zhou, J.; Yu, H.; Li, L.; Wu, H. Directing osteogenesis of stem cells with drug-laden, polymer-microsphere-based micropatterns generated by Teflon microfluidic chips. *Adv. Funct. Mater.* **2012**, *22*, 3799−3807.

(21) Kim, S.; Park, C. B. Bio-inspired synthesis of minerals for energy, environment, and medicinal applications. *Adv. Funct. Mater.* **2013**, *23*, 10−25.

(22) Fletcher, D. A.; Mullins, R. D. Cell mechanics and the cytoskeleton. *Nature* **2010**, *463*, 485−492.

(23) Lee, H.; Rho, J.; Messersmith, P. B. Facile conjugation of biomolecules onto surfaces via mussel adhesive protein inspired coatings. *Adv. Mater.* **2009**, *21*, 431−434.

(24) Lynge, M. E.; van der Westen, R.; Postma, A.; Stadler, B. Polydopamine-a nature-inspired polymer coating for biomedical science. *Nanoscale* **2011**, *3*, 4916−4928.

(25) Lee, H.; Scherer, N. F.; Messersmith, P. B. Single-molecule mechanics of mussel adhesion. *Proc. Natl. Acad. Sci. U.S.A.* **2006**, *103*, 12999−13003.

(26) Lee, H.; Dellatore, S. M.; Miller, W. M.; Messersmith, P. B. Mussel-inspired surface chemistry for multifunctional coatings. *Science* **2007**, *318*, 426−430.

(27) Lee, H.; Lee, Y.; Statz, A. R.; Rho, J.; Park, T. G.; Messersmith, P. B. Substrate-independent layer-by-layer assembly by using mussel-adhesive-inspired polymers. *Adv. Mater.* **2008**, *20*, 1619−1623.

(28) Irimia, D.; Geba, D. A.; Toner, M. Universal microfluidic gradient generator. *Anal. Chem.* **2006**, *78*, 3472−3477.

(29) Okuyama, T.; Yamazoe, H.; Seto, Y.; Suzuki, H.; Fukuda, J. Cell micropatterning inside a microchannel and assays under a stable concentration gradient. *J. Biosci. Bioeng.* **2010**, *110*, 230−237.

(30) Bellan, L. M.; Kniazeva, T.; Kim, E. S.; Epshteyn, A. A.; Cropek, D. M.; Langer, R.; Borenstein, J. T. Fabrication of a hybrid microfluidic system incorporating both lithographically patterned microchannels

and a 3D fiber-formed microfluidic network. *Adv. Healthcare Mater.* **2012**, *1*, 164−167.
(31) Gurkan, U. A.; Tasoglu, S.; Akkaynak, D.; Avci, O.; Unluisler, S.; Canikyan, S.; MacCallum, N.; Demirci, U. Smart interface materials integrated with microfluidics for on-demand local capture and release of cells. *Adv. Healthcare Mater.* **2012**, *1*, 661−668.
(32) Mizuno, J.; Ostrovidov, S.; Sakai, Y.; Fujii, T.; Nakamura, H.; Inui, H. Human ART on chip: Improved human blastocyst development and quality with IVF-chip. *Fertil. Steril.* **2007**, *88*, S101.
(33) Ostrovidov, S.; Sakai, Y.; Fujii, T. Integration of a pump and an electrical sensor into a membrane-based PDMS microbioreactor for cell culture and drug testing. *Biomed. Microdevices* **2011**, *13*, 847−864.
(34) Ostrovidov, S.; Seidi, A.; Ahadian, S.; Ramalingam, M.; Khademhosseini, A. Micro- and nanoengineering approaches to developing gradient biomaterials suitable for interface tissue engineering. In *Micro and nanotechnologies in engineering stem cells and tissues*; Ramalingam, M., Jabbari, E., Ramakrishna, S., Khademhosseini, A., Eds.; John Wiley & Sons, Inc.: Hoboken, NJ, 2013; pp 52−79.
(35) Ostrovidov, S.; Annabi, N.; Seidi, A.; Ramalingam, M.; Dehghani, F.; Kaji, H.; Khademhosseini, A. Controlled release of drugs from gradient hydrogels for high-throughput analysis of cell-drug interactions. *Anal. Chem.* **2012**, *84*, 1302−1309.
(36) Reynolds, P. M.; Pedersen, R. H.; Riehle, M. O.; Gadegaard, N. A dual gradient assay for the parametric analysis of cell−surface interactions. *Small* **2012**, *8*, 2541−2547.
(37) Shin, Y. M.; Lee, Y. B.; Kim, S. J.; Kang, J. K.; Park, J.-C.; Jang, W.; Shin, H. Mussel-inspired immobilization of vascular endothelial growth factor (VEGF) for enhanced endothelialization of vascular grafts. *Biomicromolecules* **2012**, *13*, 2020−2028.
(38) Ko, E.; Yang, K.; Shin, J.; Chi, S.-W. Polydopamine-assisted osteoinductive peptide immobilization of polymer scaffolds for enhanced bone regeneration by human adipose-derived stem cells. *Biomicromolecules* **2013**, *14*, 3202−3213.
(39) Poh, C. K.; Shi, Z.; Lim, T. Y.; Neoh, K. G.; Wang, W. The effect of VEGF functionalization of titanium on endothelial cells in vitro. *Biomaterials* **2010**, *31*, 1578−1586.
(40) Chien, C.-Y.; Tsai, W.-B. Poly (dopamine)-assisted immobilization of Arg-Gly-Asp peptides, hydroxyapatite, and bone morphogenic protein-2 on titanium to improve the osteogenesis of bone marrow stem cells. *ACS Appl. Mater. Interfaces* **2013**, *5*, 6975−6983.
(41) Ryu, J.; Ku, S. H.; Lee, H.; Park, C. B. Mussel-inspired polydopamine coating as a universal route to hydroxyapatite crystallization. *Adv. Funct. Mater.* **2010**, *20*, 2132−2139.
(42) Rivera, J. G.; Messersmith, P. B. Polydopamine-assisted immobilization of trypsin onto monolithic structure for protein digestion. *J. Sep. Sci.* **2012**, *35*, 1514−1520.
(43) Sun, K.; Xie, Y.; Ye, D.; Zhao, Y.; Cui, Y.; Long, F.; Zhang, W.; Jiang, X. Mussel-inspired anchoring for patterning cells using polydopamine. *Langmuir* **2012**, *28*, 2131−2136.
(44) Ku, S. H.; Lee, J. S.; Park, C. B. Spatial control of cell adhesion and patterning through mussel-inspired surface modification by polydopamine. *Langmuir* **2010**, *26*, 15104−15108.
(45) Chien, H.-W.; Kuo, W.-H.; Wang, M.-J.; Tsai, S.-W.; Tsai, W.-B. Tunable micropatterned substrates based on poly(dopamine) deposition via microcontact printing. *Langmuir* **2012**, *28*, 5775−5782.
(46) Wang, J.-L.; Ren, K.-F.; Chang, H.; Jia, F.; Li, B.-C.; Ji, Y.; Ji, J. Direct adhesion of endothelial cells to bioinspired poly(dopamine) coating through endogenous fibronectin and integrin $\alpha_5\beta_1$. *Macromol. Biosci.* **2013**, *13*, 483−493.
(47) Lee, S. J.; Khang, G.; Lee, Y. M.; Lee, H. B. The effect of surface wettability on induction and growth of neurites from the PC-12 cell on a polymer surface. *J. Colloid Interface Sci.* **2003**, *259*, 228−235.
(48) Genzer, J.; Bhat, R. R. Surface-bound soft matter gradients. *Langmuir* **2008**, *24*, 2294−2317.
(49) Almodovar, J.; Crouzier, T.; Selimovic, S.; Boudou, T.; Khademhosseini, A.; Picart, C. Gradients of physical and biochemical cues on polyelectrolyte multilayer films generated via microfluidics. *Lab Chip* **2013**, *13*, 1562−1570.
(50) Masters, K. S. Covalent growth factor immobilization strategies for tissue repair and regeneration. *Macromol. Biosci.* **2011**, *11*, 1149−1163.
(51) Li, B.; Ma, Y.; Wang, S.; Moran, P. M. A technique for preparing protein gradients on polymeric surfaces: Effects on PC12 pheochromocytoma cells. *Biomaterials* **2005**, *26*, 1487−1495.
(52) Miller, E. D.; Phillippi, J. A.; Fisher, G. W.; Campbell, P. G.; Walker, L. M.; Weiss, L. E. Inkjet printing of growth factor concentration gradients and combinatorial arrays immobilized on biologically-relevant substrates. *Comb. Chem. High Throughput Screening* **2009**, *12*, 604−618.
(53) Jiang, J.; Zhu, L.; Zhu, L.; Zhu, B.; Xu, Y. Surface characteristic of a self-polymerized dopamine coating deposited on hydrophobic polymer films. *Langmuir* **2011**, *27*, 14180−14187.
(54) Bernsmann, F.; Ball, V.; Addiego, F.; Ponche, A.; Michel, M.; Gracio, J. J. D. Dopamine-melanin film deposition depends on the used oxidant and buffer solution. *Langmuir* **2011**, *27*, 2819−2825.
(55) Kannan, B.; Higgins, D. A.; Collinson, M. M. Aminoalkoxysilane reactivity in surface amine gradients prepared by controlled-rate infusion. *Langmuir* **2012**, *28*, 16091−16098.
(56) Fors, B. P.; Poelma, J. E.; Menyo, M. S.; Robb, M. J.; Spokoyny, D. M.; Kramer, J. W.; Waite, J. H.; Hawker, C. J. Fabrication of unique chemical patterns and concentration gradients with visible light. *J. Am. Chem. Soc.* **2013**, *135*, 14106−14109.
(57) Lamb, B. M.; Park, S.; Yousaf, M. N. Microfluidic permeation printing of self-assembled monolayer gradients on surfaces for chemoselective ligand immobilization applied to cell adhesion and polarization. *Langmuir* **2010**, *26*, 12817−12823.
(58) Kang, S. M.; You, I.; Cho, W. K.; Shon, H. K.; Lee, T. G.; Choi, I. S.; Karp, J. M.; Lee, H. One-step modification of superhydrophobic surfaces by a mussel-inspired polymer coating. *Angew. Chem., Int. Ed.* **2010**, *49*, 9401−9404.